非晶态镍基钎料箔润湿成缝特征及其对钎焊接头形态的影响

王　君[1]，何　鹏[1]，李　军[1,2]，李钟麟[2]，钱乙余[1]
(1. 哈尔滨工业大学 先进焊接与连接国家重点实验室，哈尔滨　150001；
2. 浙江银轮机械股份有限公司，台州　317200)

王　君

摘　要：通过分析控制非晶态镍基钎料箔用量的钎焊试验结果，对非晶态镍基钎料箔的润湿成缝特征及钎焊接头形态进行了研究. 结果表明，即使在钎料不足的情形下，钎料残余层也始终存在，在熔融钎料同母材的相互作用下，钎料残余层/母材界面向母材一侧发生迁移；钎料残余层厚度随钎料量的增加而增大，但界面迁移深度与钎料箔大小无关. 熔融钎料成缝行为遵循能量最低原理，其受自身重力、粘滞力和表面张力引起的附加压力共同作用，流动成缝时具有粘性流体的特征，贴近母材表面的边界层流速趋缓，母材向熔融钎料中的溶解则进一步降低了其流动性，最终凝固形成钎料残余层.

关键词：非晶态镍基钎料箔；润湿成缝特征；接头形态
中图分类号：TG454　　**文献标识码**：A　　**文章编号**：0253－360X(2013)12－0046－04

0　序　　言

非晶态镍基钎料箔广泛应用于工业领域中不锈钢及高温合金的钎焊连接，由于制造方法的限制，非晶态镍基钎料箔厚度往往在 50 μm 以下[1,2]，因而其在微观组织形态和宏观厚度上均与普通钎料存在差异，这使得其润湿成缝过程具有自身的特点[3,4]. 然而，对于非晶态镍基钎料箔的润湿成缝特征的国内外研究较少，文中将在试验的基础上对非晶态镍基钎料箔的润湿成缝特征展开研究和分析，并就其对接头形态的影响进行探讨.

1　试验方法

试验所用母材为 204 不锈钢，分别选用了 60 mm×40 mm×2 mm 的不锈钢板和厚度为 0.5 mm、直径为 32 mm 的不锈钢环，所用非晶态钎料箔为厚 25 μm 的 BNi-5a 镍基钎料. 母材与钎料两者成分见表 1. 入炉钎焊前，先将钎料箔依照图 1 所示形式置于不锈钢环板间并使用卡具固定，试验中通过改变钎料箔的宽度 l 来控制钎料量. 钎焊在真空钎焊炉中进行，钎焊温度为 1 190 ℃，保温时间为 15 min. 钎焊后，对图 1 中距钎料近端 a 和距钎料远端 b 两处的接头成缝情况和各试样残余钎料层进行显微组织分析和能谱分析.

表 1　试验材料化学成分(质量分数，%)
Table 1　Chemical compositions of experiment materials

	Si	Mn	Cr	Ni	Fe
204 不锈钢	1.00	7.0～9.0	15.0～17.0	1.50～3.00	余量
BNi-5a	7.0～7.5	0	18.5～19.5	余量	0.5

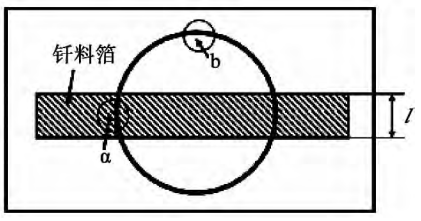

图 1　试样装配示意图
Fig. 1　Schematic of assembled method of samples

2　试验结果与讨论

2.1　钎焊圆角成形及分析

钎焊后通过显微观察发现，在各试样接头处均

收稿日期：2012－09－16
基金项目：国家自然科学基金资助项目(51275135，51021002，51105107，51305102)

形成了钎焊圆角，但圆角截面积随使用钎料量的增加而增大. 钎焊圆角外轮廓与截面积变化情况如图 2 所示. 在各试样 b 处，圆角成形情况不尽相同，如图 3 所示. 可见，使用 l 为 1 mm 和 1.5 mm 的钎料箔带时，熔融钎料并未流动至 b 处填缝形成圆角；对于形成了钎焊圆角的接头，其截面积亦随钎料箔带宽度的增加而增大.

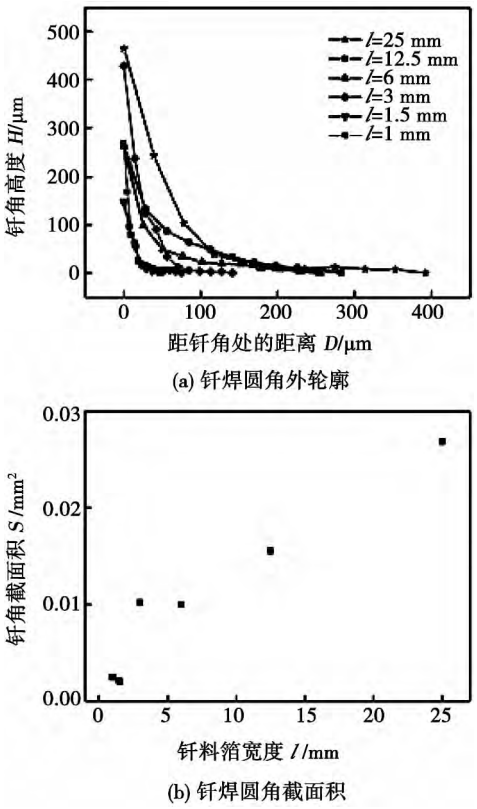

图 2　各试样 a 处的钎焊圆角外轮廓与截面积

Fig. 2　Fillet outline and sectional area at a position of samples

而将各试样的 a，b 两处钎焊圆角外轮廓线进行对比，可以发现同一试样 a 处的钎焊圆角总是大于 b 处，那么相应地，同一试样 a 处钎焊圆角的截面积也总是大于 b 处钎焊圆角的截面积. 可以认为，在一定范围内，相同条件下钎料箔的面积与钎焊圆角的截面积成正比，无论对于钎料箔片预置在钎缝中的情形还是钎料通过毛细作用成缝的情形均是如此；在钎料箔面积相同时，钎料箔预置在钎缝中的接头部位形成的钎焊圆角要比距离钎料箔较远、需要通过毛细作用成缝的部位更为饱满.

钎焊圆角的形成过程可认为是沿平行间隙的毛细填缝和熔融钎料沿环壁爬升的动态过程[5]. 当减小钎料箔带面积时，熔融钎料量相应减少. 平行间隙填缝所需的钎料量为常数，当平行间隙填缝完成、

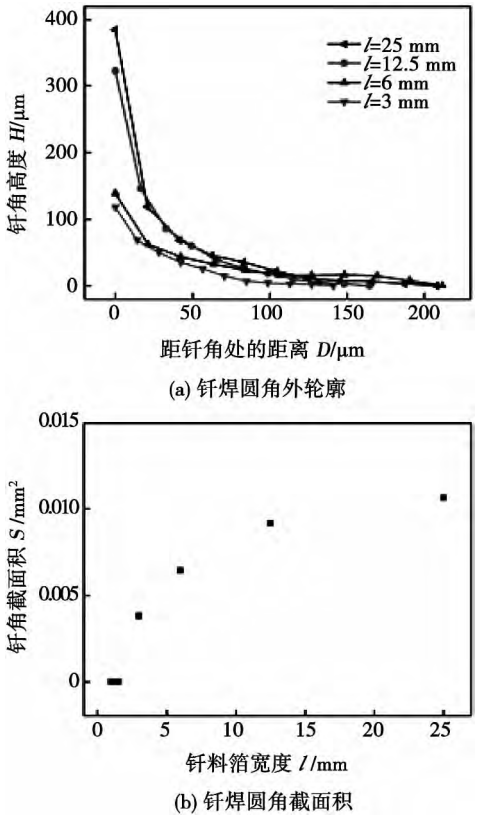

图 3　各试样 b 处的钎焊圆角外轮廓与截面积

Fig. 3　Fillet outline and sectional area at b position of samples

形成饱满钎焊圆角所需钎料量不足的情况下，钎料沿环壁爬升的过程未充分进行即在中途停止. 由于各试样所用钎料箔宽度依次减小，钎料量依次减少，故而钎料在形成钎焊圆角过程中的不同阶段停止爬升，钎焊圆角形态和截面积也呈现出了相应的递变规律.

2.2　钎料残余层的厚度变化规律

钎焊后，在 a 处接头两侧存在一层钎料残余层，而 b 处接头两侧并未出现. 事实上，观察发现存在残余钎料层的区域与先前放置钎料箔片的区域是基本吻合的. 对钎料残余层的边缘观察发现，钎料残余层与母材的界面相对于原先的母材表面发生了迁移，如图 4 所示. 经过对各试样的界面迁移深度进行测量，发现这一数值基本维持在 15 μm 左右，并不随钎料箔宽度的变化而变化；钎料残余层厚度则随着钎料箔宽度的增加而增加，见图 5.

2.3　非晶态镍基钎料箔成缝行为分析

对于熔融钎料、母材和 1×10^{-3} Pa 的真空环境所组成的封闭系统，在其达到平衡状态时应遵循能量最低原理. 对于这一体系而言，若只计入在由初始态达到平衡态过程中发生改变的能量项，则有总能量[6].

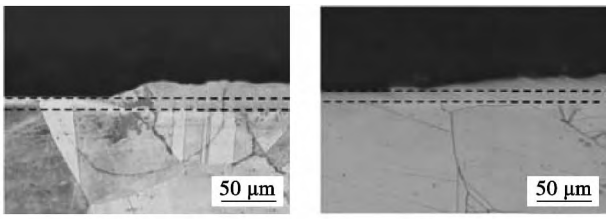

(a) l =25 mm (b) l =1 mm

图 4 钎料残余层/母材的界面迁移

Fig. 4 Migration of interface of filler metal residual layer and base metal

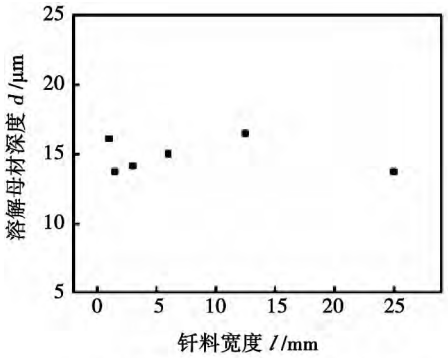

(a) 迁移深度与钎料箔宽度的关系

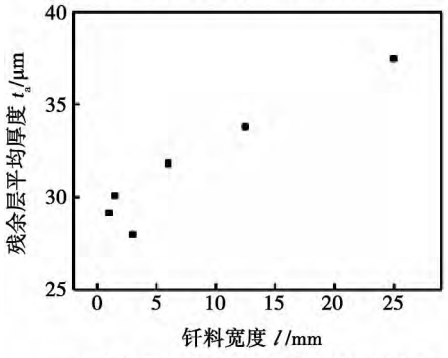

(b) 残余层平均厚度与钎料箔厚度的关系

图 5 钎料残余层/母材界面的迁移深度及残余层厚度与钎料箔宽度的关系

Fig. 5 Relation between migration depth and foil width and relation between thickness of filler metal residual layer and foil width

$$E_{\text{total}} = E_{\text{G}} + E_{\text{l-v}} + E_{\text{s-v}} + E_{\text{s-l}} \tag{1}$$

式中: E_{total} 为系统总能量; E_{G} 为熔融钎料的重力势能; $E_{\text{l-v}}$ 为熔融钎料的表面能; $E_{\text{s-v}}$ 为母材的表面能; $E_{\text{s-l}}$ 为熔融钎料与母材间的界面能.

那么当式(1)取最小值时,熔融钎料在自身重力和表面张力引起的附加压力共同作用下达到平衡形态.

钎料自发的填缝过程是系统总能量 E_{total} 下降的过程. 钎缝间隙中母材表面具有显微不平度,钎料熔化后因表面张力液面形状发生改变,在间隙小的部位钎料率先形成对两侧母材的润湿,在弯曲液面附加压力的作用下不断扩展,润湿面积增大,最终形成连续的钎料填充区域.

在模拟试验中,不锈钢环与板间的钎缝对熔融钎料存在毛细作用力,由于 a 处不锈钢环直接压在钎料箔带上,那么当钎料熔化后,熔融钎料从 a 处附近流入钎缝,并由 a 处向 b 处扩展. 倘若用于填缝的钎料量不足,那么熔融钎料在尚未流动至 b 处时就已停止. l = 1.5 mm 和 l = 1 mm 的试样 b 处便是如此.

对于某一试样 a,b 两处的钎焊圆角差异,除了 b 处钎料量不足的原因外,两处的钎料润湿方式也是存在差别的. a 处钎料箔预置在钎缝中,情况与附着润湿接近; b 处钎料流动成缝,润湿方式属于铺展润湿. 而对于附着功 W_{a} 和铺展功 W_{s},存在如下关系[5],即

$$W_{\text{s}} = W_{\text{a}} - W_{\text{n}} < W_{\text{a}} \tag{2}$$

式中: W_{n} 为液体的内聚功.

附着功 W_{a} 和铺展功 W_{s} 的物理意义为润湿过程中自由能变化 ΔG 的相反数. 相同条件下,$\Delta G < 0$ 的过程可自发进行,其中 $|\Delta G|$ 较大的过程在热力学上认为更易发生. 由式(2)可以判断,相同条件下附着润湿更易发生,这也导致了同一试样 a,b 两处的钎焊圆角出现差异.

2.4 钎料残余层形成的综合分析

当钎焊圆角不饱满甚至 b 处钎料未填缝时,钎料残余层仍然存在. 换言之,钎料残余层总是存在的,与钎缝间隙是否填满无关. 这促使了对镍基钎料箔的流动铺展过程的思考.

熔融钎料属于粘性流体. 当钎料熔化后开始流动时,其流动速度在垂直于母材表面方向上的分量很小,那么,在母材—熔融钎料界面附近,熔融钎料薄层的流动与层流边界层相似. 对于层流边界层而言,在贴近固体表面的一个薄层当中,其速度迅速降为零,在边界层中存在相当大的速度梯度. 若忽略平行于钎料箔宽度方向的速度分量,则边界层中流体的运动方程为[7]

$$\left.\begin{aligned} v_x\frac{\partial v_x}{\partial x} + v_y\frac{\partial v_y}{\partial y} - \gamma\frac{\partial^2 v_x}{\partial y^2} &= -\frac{1}{\rho}\frac{\mathrm{d}p}{\mathrm{d}x} = U\frac{\mathrm{d}U}{\mathrm{d}x} \\ \frac{\partial v_x}{\partial x} + \frac{\partial v_y}{\partial y} &= 0 \end{aligned}\right\} \tag{3}$$

式中: v_x 为熔融钎料水平方向上的速度分量; v_y 为熔融钎料竖直方向上的速度分量; γ 为运动粘性系数,$\gamma = \eta/\rho$,η 为动力粘性系数; p 为主流对边界层的压力; U 为主流的速度. 由于边界层与主流区域的边界并不十分明显,在计算时可将熔融钎料一定

厚度的表层作为主流区域.

将熔融钎料流动看作是包含层流边界层的流动行为的话，钎料残余层始终存在的现象便不难理解了. 由于母材表面并非光滑表面，且熔融钎料与母材之间有着强烈的相互作用，因此随着 y 值减小，熔融钎料流动逐渐变慢，贴近母材表面的熔融钎料薄层流动速度趋近于零. 在钎焊后冷却阶段，残留的熔融钎料凝固结晶，形成了钎料残余层.

对于边界层的厚度 δ，有[7]

$$\delta \propto \frac{L}{\sqrt{Re}} \tag{4}$$

式中：L 为特征长度，为常数；Re 为雷诺数，$Re = \rho v L/\eta$. 由式(4)可以看出，当熔融钎料粘度增大、流动性变差时，边界层厚度 δ 也随之增大.

以钎料箔宽度为 12.5 mm 的试样为例，对其钎料残余层及附近区域进行线扫描及能谱点分析. 图 6 中竖实线为钎料残余层与母材的分界线，在其两侧根据元素含量的变化可划分出 I，II，III 三个区域.

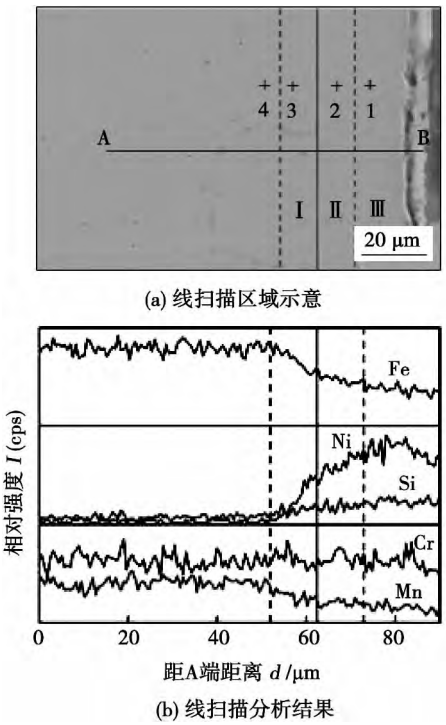

图 6　钎料残余层及附近区域的线扫描分析

Fig. 6　Linear EDS analysis of filler metal residual layer and nearby area

I 区域宽约 11 μm，为母材靠近钎料层的镍，硅扩散区，在这一区域内 Ni，Si 元素含量呈现出钎料层—母材方向的正向浓度梯度，而此区域内 Fe，Mn 元素的浓度梯度方向与之相反. 对点 3 处能谱分析，Fe 60.34%，Ni 15.35%，而母材点 4 处的 Fe 72.61%，Ni 0.90%，可见 Ni 元素扩散使得 I 区域成分有了很大改变. II 区域宽约 12 μm，为母材在钎料残余层中的溶解区，该区域中各元素的浓度变化趋势与镍、硅扩散区相同，但浓度梯度较小，这说明在熔融钎料中元素扩散进行得更为充分. III 区域为钎料残余层外层，各元素含量较为稳定. 可以认为，钎料残余层与母材的界面迁移是由于熔融钎料与母材的相互作用而引起的，主要是母材向熔融钎料中的溶解. 对图 6a 中点 1、点 2 处分别进行能谱分析，点 1 处 Fe 30.61%，Ni 44.61%；点 2 处 Fe 35.52%，Ni 40.49%. 可见，母材的溶解深刻地影响了钎料残余层的成分，残余钎料已由 Ni-Cr 合金转变为 Ni-Fe-Cr 合金，使得熔融钎料粘度增大，流动性变差.

3　结　　论

(1) 在熔融钎料同母材的相互作用下，钎料残余层始终存在，且钎料残余层/母材界面向母材一侧发生迁移. 试验中钎料残余层厚度随钎料用量的增加而增大，但界面迁移深度与钎料箔大小无关.

(2) 熔融钎料成缝行为遵循能量最低原理，总能量最低时，熔融钎料在自身重力、粘滞力和表面张力引起的附加压力共同作用下达到平衡状态.

(3) 熔融钎料流动成缝时具有粘性流体的特征，贴近母材表面的边界层流速趋缓，母材向熔融钎料中的溶解则进一步降低了其流动性，最终凝固形成钎料残余层.

参考文献：

[1] 张贵锋，张建勋，裴　怡，等. Ni 基及 Fe 基非晶态箔带钎料对碳素钢管的润湿行为[J]. 焊接学报，2006，27(7)：61－64.
Zhang Guifeng，Zhang Jianxun，Pei Yi，*et al*. Wetting behavior of nickel based and iron based amorphous filler metal foil on plain carbon steel pipe[J]. Transactions of the China Welding Institution，2006，27(7)：61－64.

[2] Wang B，Zhu T，Dong F，*et al*. Preparation and properties of a custom-designed nickel-based amorphous brazing foil[J]. Advanced Materials Research，2012，499：143－146.

[3] 张　勇，张国庆，何志勇，等. Cr 与 B 对镍基高温钎料在 C_f/SiC 陶瓷基复合材料上润湿性的影响[J]. 焊接学报，2007，28(12)：93－96.
Zhang Yong，Zhang Guoqing，He Zhiyong，*et al*. Influence of chromium and boron on wettability of nickel-based high temperature filler metal on C_f/SiC ceramic matrix composite[J]. Transactions of the China Welding Institution，2007，28(12)：93－96.

[下转第 54 页]

[5] Kou S. Welding Metallurgy [M]. Ann: industry press, 1987.

[6] 徐国建，殷德洋，杭争翔，等. 激光堆焊 Co 基合金与 VC 混合粉末组织和性能 [J]. 沈阳工业大学学报，2012，34(1)：26－30.
Xu Guojian, Yin Deyang, Hang Zhengxiang, *et al*. Microstructure and property of laser overlaid layer of mixed Co-based alloy and VC powder [J]. Journal of Shenyang University of Technology, 2012, 34(1): 26－30.

[7] 戚文军，何艳兵，刘 斌，等. 激光堆焊镍基碳化钨梯度焊层及耐磨机理分析 [J]. 焊接学报，2002，23(1)：57－60.
Qi Wenjun, He Yanbing, Liu Bin, *et al*. Gradient hardfacing on the laser overlay deposit tungsten carbide of the nickel matrix and wearable mechanism analyze [J]. Transactions of the China Welding Institution, 2002, 23(1): 57－60.

[8] Savage W F. Welding in the World [J]. Material Science and Engineering, 1980, 18(5/6): 89－114.

作者简介： 徐国建，男，1959 年出生，博士，教授. 主要从事先进激光制造装备及加工工艺等方面的研究. 发表论文近 50 篇. xuguojian1959@ hotmail. com.

[上接第 49 页]

[4] 叶 雷，李晓红，毛 唯，等. Hf 与 Zr 为降熔元素镍基钎料对 IC10 合金的钎焊 [J]. 焊接学报，2009，30(2)：137－140.
Ye Lei, Li Xiaohong, Mao Wei, *et al*. Brazing of IC10 superalloy with Ni based brazing fillers using Hf and Zr as melting-point depressants [J]. Transactions of the China Welding Institution, 2009, 30(2): 137－140.

[5] 方洪渊，冯吉才. 材料连接中的界面行为 [M]. 哈尔滨：哈尔滨工业大学出版社，2005.

[6] 高 峰. 铝热交换器复合钎料板钎焊接头成型机理研究 [D]. 哈尔滨：哈尔滨工业大学，2003.

[7] Landau L, Lifscitz E. 理论物理学教程第六卷：流体力学 [M]. 北京：高等教育出版社，2009.

作者简介： 王 君，男，1988 年出生，博士研究生. 主要从事材料连接机理方面的研究工作. 已发表论文 5 篇. Email: dtvir@126. com

通讯作者： 何 鹏，男，教授，博士研究生导师. Email: hithepeng@ hit. edu. cn

Key words: coupling arc electrode; arc pressure; weld shape; high-speed welding

Effect of pulse frequency on weld appearance behavior of TC4 titanium alloys YANG Zhou, QI Bojin, CONG Baoqiang, YANG Mingxuan, LI Yulong (School of Mechanical Engineering and Automation, Beihang University, Beijing 100191, China). pp 37 - 40

Abstract: An experimental of weld penetration of TC4 titanium alloys was carried out by using ultrahigh frequency pulse-tungsten inert gas welding process. The effect of pulsed current frequency on weld appearance was investigated. The experimental results show that when pulse frequency f ≤65kHz, the variation of welds depth and width with the increment of pulse frequency are basically the same trend, and compared with conventional GTAW process, the weld width decreased by more than 12%. In the range of 20 ~ 40 kHz, the weld depth-to-width ratio increases obviously, while it tends to be stable with further increase of pulse frequency. The weld width decreases approximately by 35% as pulse frequency is higher than 70 kHz. Meanwhile, the weld depth increases slightly and the depth to width ratio can be enhanced strikingly with ultra-high frequency. Based on the data from experiment of arc profile, the most dominant mechanism for the variation of weld appearance can be considered as arc constriction caused by pulse frequency.

Key words: ultra-high frequency pulse GTAW process; weld appearance; arc constriction

Eccentric extrusion flow model of friction stir welding DENG Yongfang[1,2], ZUO Dunwen[1,2], SONG Bo[1,2] (1. College of Mechanical & Electrical Engineering, Nanjing University of Aeronautics and Astronautics, Nanjing 210016, China; 2. Jiangsu Key Laboratory of Precision and Micro-manufacturing Technology, Nanjing 210016, China). pp 41 - 45

Abstract: The eccentric extrusion flow model of friction stir welding was proposed. The model shows that the eccentric extrusion effect of tool for softening material is the most important factor for the formation of joint. The tool with eccentric structure was designed and friction stir welding experiments were carried out, and the influence of the eccentricity of tool on material flow was analyzed. Research shows that the joint forms by the tool eccentrically extruding material in the friction stir welding process. The greater the eccentricity of the tool is, the larger the weld nugget zone of the joint is. Metal flow near the pin will form the relatively obvious layered structure in the advancing direction. The arc lines will form on the surface of the weld, which are not symmetrical, but turn to the retreating side. Angle formed in the retreating side is larger than that formed in the advancing side in the arc lines. There is a corresponding relationship between the layered structure in the advancing direction and arc lines on the surface of the weld.

Key words: friction stir welding; eccentricity; extrusion; flow model

Wetting and joint-formed characteristics of amorphous Ni-based filler metal foil and its influence on brazed joint formation WANG Jun[1], HE Peng[1], LI Jun[1,2], LI Zhonglin[2], QIAN Yiyu[1] (1. State Key Laboratory of Advanced Welding and Joining, Harbin Institute of Technology, Harbin 150001, China; 2. Zhejiang Yinlun Machinery Co., Ltd., Taizhou 317200, China). pp 46 - 49, 54

Abstract: The control of the amount of amorphous nickel-based filler metal foil was analyzed, and the wetting and joint-formed characteristics of the amorphous nickel-based filler metal foil and brazed joint formation were studied. The results showed that the filler metal residual layer always exists after the brazing process with amorphous nickel-based filler metal foil, even when the filler metal is insufficient to fill in the joint. The migration of the interface between filler metal residual layer and base metal was observed, which was related to the interaction between molten filler metal and base metal. The thickness of filler metal residual layer increases with adding the filler metal foil, but the interface migration depth does not relate to the filler metal foil size. The joint-formed behavior of molten filler metal follows the minimum energy principle, the molten filler metal is affected by its own gravity, viscous force and the additional pressure are caused by surface tension, which flow into the seam with viscous fluid characteristics. The flow rate of liquid alloy in the boundary layer closing to steel surface gradually slows down, and the dissolution of base metal to the molten filler metal further reduces its fluidity. Finally the molten filler metal solidifies and the residual layer forms.

Key words: amorphous nickel-based filler metal foil; wetting and joint-formed characteristics; joint shape

Properties of Ni-based alloy powder cladding layer by CO_2 laser beam and plasma XU Guojian[1], DONG Shilong[1], HANG Zhengxiang[1], ZHANG Yifei[2], LI Yongbo[2], KUTSUNA Munaharu[3] (1. Shenyang University of Technology, Shenyang 110870, China; 2. Shenyang XinSong Robotic Automation Co., Ltd., Shenyang 110168, China; 3. The Latest Laser Technology Research Center, Ann City 446-0026, Japan). pp 50 - 54

Abstract: To improve the properties of SUS316LN stainless steel in power plant part, a cladding layer was deposited on the surface of SUS316LN stainless steel by laser cladding and plasma cladding. The cladding layer was analyzed by the laser microscope, scanning electronic microscope (SEM) and X-ray diffraction (XRD), electronic probe (EPMA) and energy dispersive spectrometer (EDS). The results indicate the cladding layer belongs to hypereutectic structure. Primary phase is made of boride (CrB) and carbide (Cr_7C_3), and eutectic structure is made of γ-Ni + CrB or γ-Ni + Cr_7C_3. Compared with plasma cladding layer, the CO_2 laser cladding layer has higher wear resistance, smaller microstructure, lower dilution and higher cladding efficiency.

Key words: laser cladding; plasma cladding; hypereutectic structure; eutectic structure; primary phase

Effect of square wave loading on fatigue crack growth behavior of 20CrMo steel weld seam CHEN Xiaowen[1], ZHANG Defen[1], WANG Jian[2], LI Zengzhen[2], SHI Shuangshuang[1], WANG Jin[2], SHI Taihe[3] (1. School of Materials Science and Engineering, Southwest Petroleum University, Chengdu 610500, China; 2. School of Graduate, Southwest Petroleum U-